Heliyon 10 (2024) e40888

Contents lists available at ScienceDirect

Heliyon

journal homepage: www.cell.com/heliyon

Research article

Spatiotemporal dynamics of geomorphology, landuse, and storm surge inundation of FDMN settled in Bhasan Char island using geo-spatial techniques

Mubtasim Ishraq Antoo [a], Md. Bodruddoza Mia [a,*], Md. Asif Hasan [a,b], Mahfuzur Rahman Khan [a], Pavel Khan [a], Tareq Chowdury [a], Anupom Hasib Rose [a], Kazi Matin Uddin Ahmed [a]

[a] Department of Geology, University of Dhaka, Dhaka, 1000, Bangladesh
[b] Department of Earth and Environmental Sciences, Tulane University, USA

ARTICLE INFO

Keywords:
Geomorphology dynamics
Landuse
Storm surge inundation
Satellite image
FDMN settled in bhasan char island

ABSTRACT

Bhasan Char has undergone noteworthy transformations in its geographical characteristics since its emergence in 2003. Driven by sediment transported by the Ganges-Brahmaputra-Meghna river system, the island has gradually transitioned from a stretched-out configuration to a more rounded shape primarily due to continuous accretion, while erosion has been minimal since 2012. Currently, the island is being prepared to accommodate over 1 million Forcefully Displaced Myanmar Nationals (FDMN) refugees. This investigation, conducted over the time frame spanning from 2003 to 2023, utilizes multi-temporal satellite imagery to scrutinize the altering geography of the island, encompassing the processes of erosion and accretion, modifications in the coastline, and changes in land utilization and coverage influenced by seasonal variations. By employing the Advanced Land Observing Satellite (ALOS)/Phased Array Type L-Band Synthetic Aperture Radar (PALSAR), the study pioneers an evaluation of storm surge risks that are specific to this island. Additionally, the research utilizes water indices to understand the seasonal geomorphic dynamics of the island and performs a supervised classification to assess land utilization and coverage alterations. The inundation map shows accretion in the north and erosion in the south and southeast. Southwest is the most stable area with the majority population. After the 'Ashrayan -3′ project, significant land use and land cover changes occurred, including urbanization, embankment construction, and agricultural modifications. The average elevation of the island is 2.84 m above sea level, with a risk of inundation from storm surges exceeding 3 m. Rehabilitated populations are particularly threatened if the embankment height of 4.8 m is surpassed. The study's outcomes indicate that other projects worldwide might use the island restoration efforts as a model. This emphasizes how crucial it is to keep an eye on changes in land cover and use for upcoming planning and adaptation initiatives. Moreover, it highlights the necessity of proper assessments of storm surge hazards to guarantee the security and longevity of island communities.

* Corresponding author.
E-mail address: bodruddoza@du.ac.bd (Md.B. Mia).

https://doi.org/10.1016/j.heliyon.2024.e40888
Received 15 September 2024; Received in revised form 30 November 2024; Accepted 2 December 2024
Available online 3 December 2024
2405-8440/

1. Introduction

The coastal region of Bangladesh, particularly its low-lying islands, is highly vulnerable to coastal flooding and storm surges due to its geographic location, topography, and extreme wet weather conditions. The 'Bhasan Char' or 'floating island' is a flat piece of land formed within the southeastern end of the Bay of Bengal (BoB) 20 years ago by moving silt at the end of the Meghna River estuary. The land mass was one of the several movable, unstable islands, or "chars," that naturally exist in the area that is located 30 km off of the coast, close to the Hatiya Upazila, around 6 km from Sandwip Island and 60 miles from the mainland (The Bhasan Char Relocation Project, The Sentinel Project, 2020). Only in 2006 did the Bhashan Char-deposited river silt resurface [1]. The island was formed by Himalayan silt in 2006 and it spans 83 km^2. Over 1 million Forcefully Displaced Myanmar Nationals (FDMN) refugees are being accommodated in Bangladesh [1], having left the Rakhine state of Myanmar to flee genocide, war crimes, and severe crimes against humanity [2]. At the moment, they are crammed into congested temporary settlements with an average density of 40,000/km^2. The camps in the Cox's Bazar district are very susceptible to landslides, cyclones, and flash flooding [3]. In light of the surrounding circumstances, the government of Bangladesh recently decided to carry out the "Ashrayan - 3″ project, which entails the relocation of 100, 000 FDMN to Bhasan Char, a lonely and soiled island floating in the Bay of Bengal [Fig. 1]. The susceptibility of an island to various risks and the threat to its natural resources determines its environmental sustainability [4–10]. The sustainability of Bhasan Char for human habitation is questionable, and storm surges and rising sea levels could have a significant impact [11]). A previous study has already found a connection between an island's natural stability and secure human occupancy on a global scale [12].

Numerous studies have explored geomorphological changes and flood vulnerability within the Bay of Bengal region, particularly islands such as Nijhum Dwip, Hatia, and Sandwip, which are situated in the dynamic Meghna Estuary [13–17]. This region experiences constant erosion and accretion, heavily influenced by the Ganges-Brahmaputra-Meghna (GBM) river system, tides, and storm surges. On top of that, given the existing coastal dynamics, vulnerability to sea-level rise, and frequently occurring cyclones, the southern part

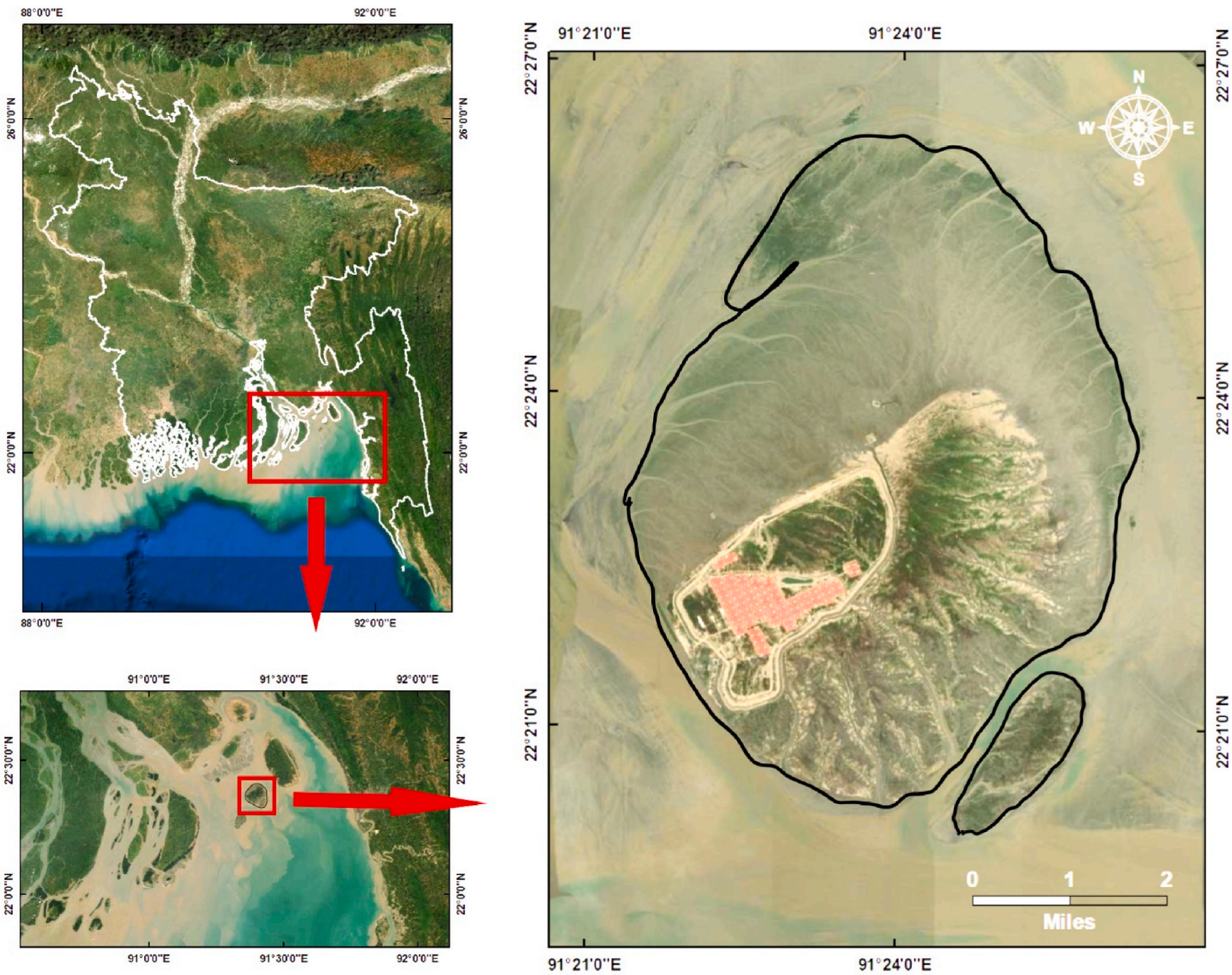

Fig. 1. Location map of the study area (Bhasan Char, Bangladesh). Background is the Google Earth map of the study area, located at south-central coastal region of Bangladesh (22°22′23.87"N; 91°22′52.28"E).

of Bangladesh is highly susceptible to climate change effects, impacting the coastal community's livelihood. Intense flooding, such as in 1987, 1988, and 1998, submerged 60 % of the nation, a trend expected to continue with a potential 40 % inundation of southern productive land by 2080. Remote sensing and Geographic Information System (GIS) techniques have been extensively used in this region to monitor coastal erosion, accretion, and flooding patterns. For instance, Hasan et al. [15] analyzed the morphological changes of Nijhum Dwip, demonstrating how alternating erosion-accretion dynamics have reshaped the island over the past two decades. Similarly, studies such as those by Bushra et al. [18] and Roy and Mahmood [19] have quantified shoreline shifts and the increasing vulnerability to storm surges. But no detailed study has taken place to investigate scenarios for Bhasan Char yet. Although [12], studied the spatiotemporal changes of this island's geomorphology and erosion-accretion, there was lack of the seasonal variations that can determine the stability of the island. While relocating the population of such magnitude, it is crucial to assess the island's resilience to natural or anthropogenic disasters to prevent catastrophic damages that can put the life of the dwellers in danger [20]. Therefore, a thorough investigation is essential to understanding the stability and evolution of the geology and geomorphology of the Bhasan Char at current state. Also, an overall assessment of the spatiotemporal change of landuse and susceptibility to storm surge inundation study is required.

Seasonal variations are extreme in Bhasan Char, being an environmentally sensitive active region. In current coastal situations, the coastline regularly shifts due to the land-water contact [15,21,22]. To comprehend these changes over longer period, or to identify the recurring cycles time series analysis using multi-temporal satellite images is a great option. Spatial modeling utilizing information from geographic information systems (GIS) and remote sensing is required for monitoring coastal dynamics [15,23]. The structural dynamics and changes in land use and cover of coastal regions can be better understood by applying water indices like the Normalized Difference Water Index (NDWI) and Modified Normalized Difference Water Index (MNDWI). Through this study we aimed at examining the seasonal morphological dynamics of Bhasan Char from 2003 to 2022 using water indices such as NDWI and MNDWI, with an emphasis on shoreline modifications, regional changes, land alterations, and erosion-accretion processes. A spatiotemporal assessment of the island's land use and an analysis of the Digital Elevation Model (DEM) to determine storm surge flooding threats are also included in the research. In addition, we intend to determine the links between land use practices, changes in land cover, and the ongoing morphological dynamics. The major focus is surely, but not limited to evaluating the spatiotemporal shift of morphological dynamics, how land use has changed historically, and how vulnerable the island is to storm surges.

The study emphasizes the necessity of considering geology, coastal dynamics, and environmental threats to determine island stability, referencing prior research on erosion-accretion processes. It also considers the critical assessment of hazard vulnerability within the island, particularly due to possible flood caused by storm surges and on the relocation of FDMN. By examining geo-environmental hazards and computing resilience, the research will aid policymakers in FDMN rehabilitation decision-making. Finding the research underscore the critical need for continuous monitoring to inform and update coastal management strategies. The results will surely help Bangladeshi officials solve issues regarding the FDMN's transfer to Bhasan Char Island, as well as, will provide significant supporting information for future research carried out by academics.

2. Study area

2.1. Location

Bhasan Char is located in the Hatiya Upazila of the Noakhali district in Bangladesh. The island is 24 km from Hatiya, 5 km from Sandwip Island, and 60 km from the mainland. Geographically, it stretches from latitudes 22°20′ to 22°27′ and longitudes 91°21′ to 91°27’ [Fig. 1]. The entire area is roughly covering 85 km^2 with an average elevation of 2.84 m above mean sea level. Currently, a 4.8 m embankment surrounds the infrastructure and settlement of the area to resist storm surge inundation.

The average monthly temperature on the island is between 27 and 38°, while the biggest amount of rainfall (333 mm) falls in July and the lowest amount (2.15 mm) falls in January. The monthly winds vary from 7.7 kmph in January to 19.7 kmph in June, while the humidity ranges from 39 % to 84 %. The range of average pressures is 1000.6–1014 MB. Because of riverine flow, wave height averages 0.5 m from January to March and peaks at 1.22 m in May. Parts of the island are covered with grass and bushes, but the island's perimeter has mangrove forests [24]. In 2003, 2008, 2013, and 2018, the percentages of vegetation on Bhasan Char were 91 %, 89 %, 88 %, and 83 %, respectively. However recent buildings to accommodate the growing settlement caused vegetation to be cleared, bringing the percentage down to 69 % in 2023.

Since October 2017, the government of Bangladesh has been developing a relocation site for 100,000 of the FDMN (Human Rights Watch, 2021). The Bangladeshi government has overseen the construction of concrete housing structures, flood defense embankments, cyclone shelters, prefabricated food and storage warehouses, roads, and a solar power grid. The first two groups, totaling about 4000 Rohingyas, had already been sent to the island between December 2020 and January 2021 (Aljazeera, 2021). As of May 2022, the Government of Bangladesh has relocated approximately 28,000 Rohingyas to Bhasan Char (WFP, 2023) The livelihood of the inhabitants of the island, that is, the Rohingyas depend on agricultural activities, garments, and employment under NGOs and government funding.

2.2. Geological setting

The Bhasan Char is situated in the Bengal Basin tectonically which is near the Barisal gravity high and east of the Hatiya trough. The land mass emerged out of the sea as one of the many shifting, unstable islands, or 'chars' that naturally occur in the region [25]. A flat land appeared twenty years ago as a result of silt accumulation. The island has gentle sand dunes with leeward and windward slopes,

Table 1
Used Satellite Images in this study.

Sensor Platform	Sensor	Acquisition Date	Spatial Resolution (m)	Season
Landsat 5	Thematic Mapper (TM)	12/9/2003	30	Post-Monsoon
		18/12/2003		Winter
		14/3/2003		Spring
		23/9/2008		Post-Monsoon
		30/12/2008		Winter
		26/3/2008		Spring
		7/5/2008		Pre-Monsoon
Landsat 8	Operational Land Imager (OLI)	28/10/2013		Post-Monsoon
		29/12/2013		Winter
		4/3/2013		Spring
		18/5/2013		Pre-Monsoon
		7/10/2018		Post-Monsoon
		24/12/2018		Winter
		17/3/2018		Spring
		26/4/2018		Pre-Monsoon
		19/102022		Post-Monsoon
		24/122022		Winter
		8/32022		Spring
		18/5/2022		Pre-Monsoon
		24/32023		Spring
DEM	ALOS PALSAR	2011	12.5	

and its landscape is a gently sloping sand flat. The major lithology is made up of silt and medium-grained sand that are dated by the Holocene. Numerous creeks, canals, and tidal channels that aid in drainage are dotted around the island. This area's tidal pattern has a semidiurnal rhythm.

3. Materials and methods

3.1. Acquisition of satellite image

Satellite images were selected for a study to analyze seasonal variations' impact on the Bhasn Char Island's geomorphologic features such as erosion-accretion, island's shape, area, landuse-landcover and shoreline conditions. Four seasons—pre-monsoon, post-monsoon, winter, and spring—were distinguished between 2003 and 2023. The island's morphology is influenced by several variables that fluctuate with the seasons, such as temperature swings, the effect of waves and tides, fluctuations in the local sea level, and morphological changes in nearby water bodies. Several factors, including tidal range, image quality, cloud cover, and other atmospheric impacts, had to be taken into account while choosing the dates for image acquisition for the study.

Multi-temporal Landsat satellite images (Landsat MSS, TM, ETM+, and OLI-TIRS) were used to analyze the dynamics and stability of Bhasan Char Island (Table 1). Utilizing Landsat images from 2003 to 2023—four images annually, spaced five years apart—seasonal fluctuations in area, shoreline, and land use-land cover were examined. With less than 10 % cloud cover for images taken during the dry season and 25–30 % cloud cover for satellite images taken during the wet season, the data was provided by the United States Geological Survey (USGS). A Digital Elevation Model (DEM) with a resolution of 12.5 m was also used in the investigation to assess the storm surge inundation. It was produced using 2011 Advanced Land Observing Satellite (ALOS)/Phased Array Type L-Band Synthetic Aperture Radar (PALSAR) data (Table 1).

3.2. Satellite image analysis

3.2.1. Geospatial software

Two main geospatial software have been used in this study for data analysis such as ArcMap 10.8 and ERDAS Imagine 9.2. ArcMap is a geographic information system (GIS) for working with maps and geographic information [26]. This software was primarily intended for use in the following areas: mapping creation and utilization; collecting and analyzing geographic data; sharing and discovering geographic information; using maps and geographic data in a range of applications; and managing geographic data global databases. ERDAS Inc. developed the remote sensing and raster graphics editor ERDAS Imagine 9.2. It helps users handle geospatial raster data and prepare, show, and improve digital images for usage in CAD or GIS software.

3.2.2. Indices used to retrieve geomorphic features

The downloaded satellite images are saved in the GeoTIFF format with the Universal Transverse Mercator (UTM) zone 46N projection and the World Geodetic System (WGS1984) datum. In ERDAS IMAGINE 9.2, each scene's component bands have been layered initially without the thermal band and band 1. A subset operation has been carried out to obtain a certain study region. To boost the image quality, radiometric and atmospheric correction have been used. By considering the specific image dates obtained from the table, erosion lines have been drawn for each of the corresponding images [Fig. 2].

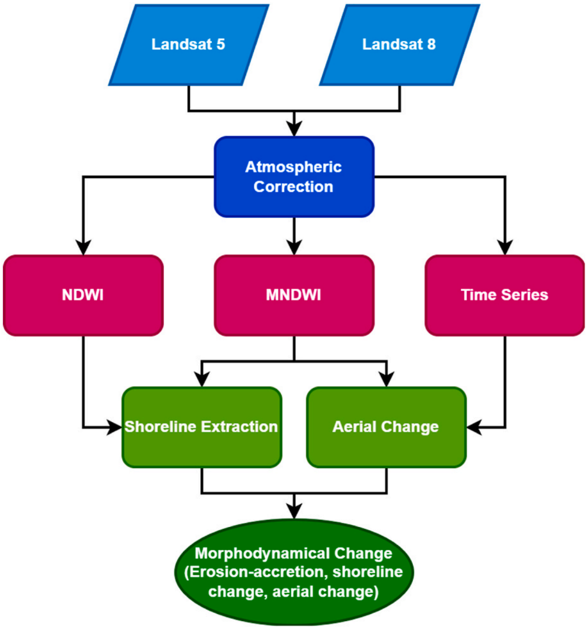

Fig. 2. Workflow of Morpho dynamics analysis of the Bashan Char Island.

Since shorelines are the most dynamic features on the planet and change quickly, accurate shoreline extraction is challenging [27]. There are numerous techniques for extracting shorelines, such as the automated Water Index Method. The study employed the Normalized Difference Water Index (NDWI) by McFeeter and the Normalized Difference Water Index (NDWI) by Xu for TM, ETM + [28,29]. Modification of Normalized Difference Water Index (MNDWI) used for OLI sensor [29]. NDWI for MSS and TM sensors was retrieved using the reflectance value of green and near infrared band according [28] [Equation (1)]:

$$NDWI = \frac{Green - NIR}{Green + NIR} \tag{1}$$

Consequently, it is possible to infer the shoreline from the contrast between land and water. Xu's MNDWI retrieval formula using the reflectance value of green and mid-infrared bands for TM and ETM + sensors [Equation (2)]:

$$MNDWI = \frac{Green - MIR}{Green + MIR} \tag{2}$$

Xu's MNDWI formula for the OLI sensor is expressed as below [Equation (3)], where the reflectance value of green and shortwave infrared bands:

$$MNDWI = \frac{Green - SWIR}{\mathrm{Green} + \mathrm{SWIR}} \tag{3}$$

When it comes to (extracting the boundary between land and water, Xu's MNDWI is more useful [30]. Minor manual error repairs were implemented when the shoreline became automated [31]. The image threshold value distinguishes the two classes. Threshold settings for McFeeters' and Xu's NDWI and MNDWI are often set to zero because the automated technique was used in this work to extract coastline [28,29]. But sometimes it needs to adjust the threshold for more accurate water bodies' delineation (Ji et al., 2009). Classification with a threshold value of the NDWI and MNDWI of TM, ETM+, and OLI images provided sharp edges between land and water. They are drawing a vector of the edges from the images allowing for the extraction of the island area at various time intervals. ArcMap 10.8 has been used to compute the extent of the island after vectors were derived from imageries for the appropriate seasons and years. By deducting the value of the prior year from the value of the current year, area and shoreline growth were computed. Area loss is represented by negative values. During a field investigation, GCPs were gathered by GPS from various land covers (waterbodies, vegetation, grassland, settlement, and agriculture) to validate the satellite images.

3.2.3. Landuse-landcover (LULC) retrieval

This work employed a supervised image classification method for Land Use-Land Cover (LULC) classification to map land cover across several years using Landsat 5 TM and Landsat 8 OLI satellite imagery [Fig. 3]. Supervised image classification is a method that assigns every image pixel to distinct classes based on labeled training samples informed by existing information of the research area. In the Pre-Processing stage, essential corrections are applied to improve the raw satellite data quality. Both datasets undergo radiometric correction to adjust for sensor errors and atmospheric correction to eliminate distortions caused by atmospheric particles. After

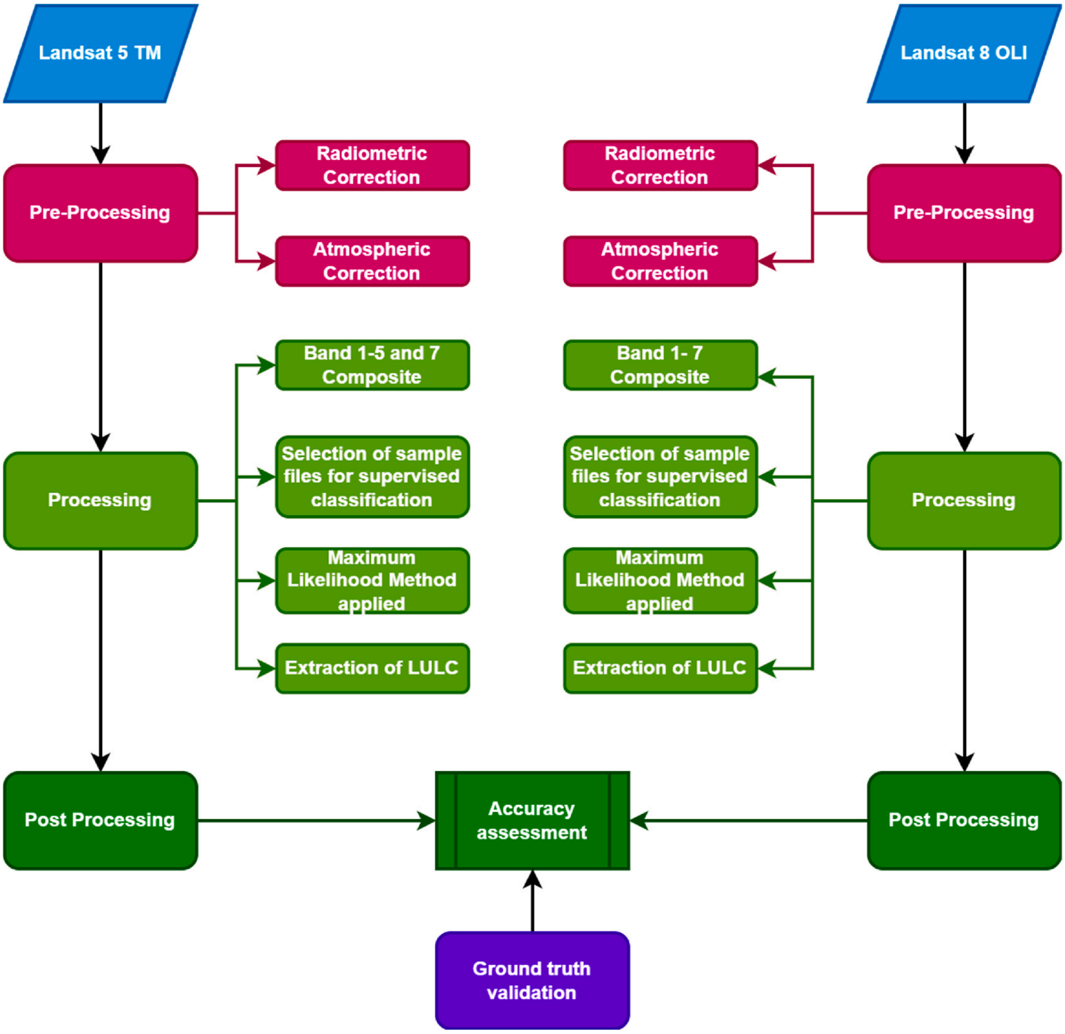

Fig. 3. Methodology workflow of LULC assessment.

corrections, composite images are prepared. For Landsat 5 TM, bands 1–5 and 7 are combined, while for Landsat 8 OLI, bands 1–7 are used. These composites serve as the input data for further analysis. During this processing phase, training samples were generated by finding and clustering pixels with analogous spectral characteristics according to their visual attributes. Subsequent to the production of the training samples, the Maximum Likelihood Classification (MLC) method was utilized to categorize pixels into established classifications. The study area was categorized into six principal land use and land cover (LULC) classes: (1) Vegetation, encompassing all forms of dense and sparse flora, including trees, shrubs, and forests; (2) Settlement, comprising all residential and urban development zones; (3) Agriculture, denoting croplands and cultivated regions; (4) Grassland, indicating areas predominantly occupied by grasses and herbaceous plants; (5) Mangrove, representing coastal wetland vegetation primarily consisting of mangrove species; and (6) Waterbody, incorporating rivers, ponds, and other aquatic features. An extensive fieldwork was conducted to acquire the actual ground data of LULC classes to carry out the post-processing phase that evaluates the accuracy of the classification by comparing the classified data with ground truth validation points, ensuring reliability and precision in the classification results. This categorization method offers an in-depth knowledge of the geographical distribution and composition of land cover categories, as well as the type of ongoing interactions within natural and anthropogenic landscapes in the studied region.

3.2.4. Surge inundation mapping

Storm surge inundation in Bashan Char is influenced by various environmental factors including atmospheric pressure, tides, and river discharge. To assess this, we utilize a geospatial approach combining digital elevation models (DEM) with cyclone frequency analysis and coastline vector data [15,32]. The DEM provides detailed terrain information, including elevation, slope, and flow direction, essential for understanding how water moves during storm surges. Historical cyclone data is analyzed to determine surge heights for different return periods, considering factors like wind direction, distance from shore, and the frequency of past storm events. From the DEM, terrain is classified into elevation zones, with low elevation areas polygonized to represent regions susceptible

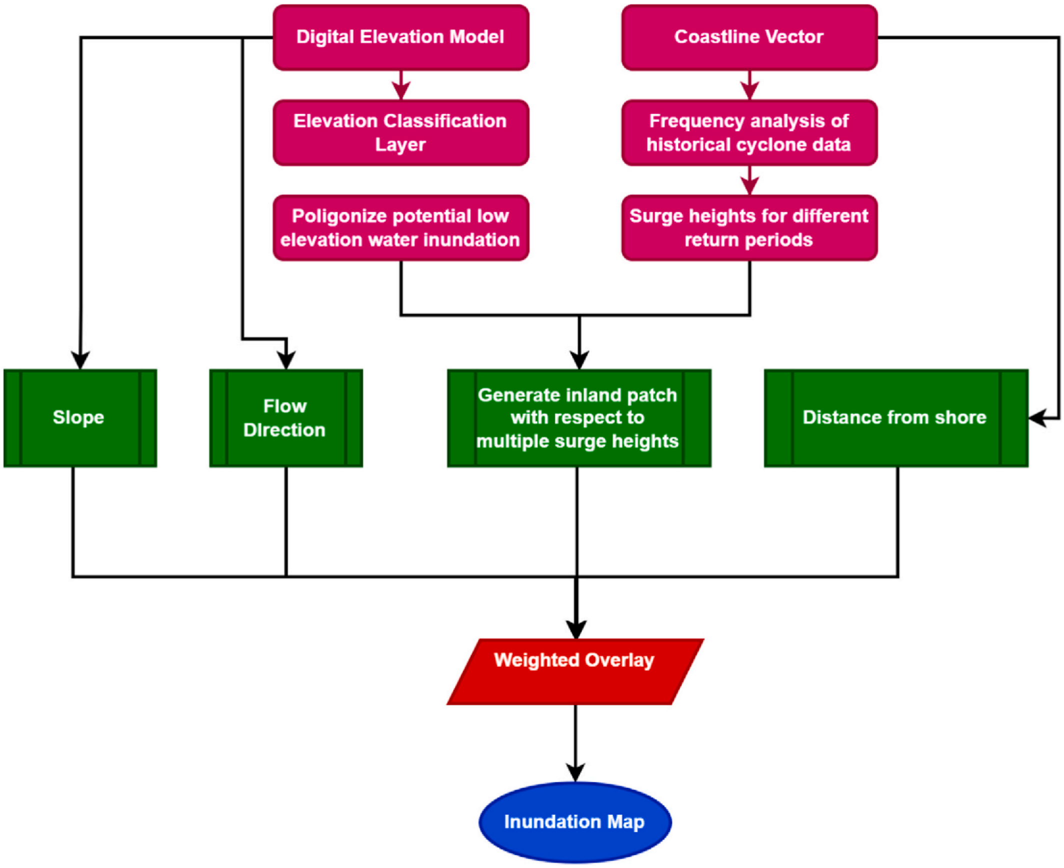

Fig. 4. Methodology workflow for storm surge inundation mapping.

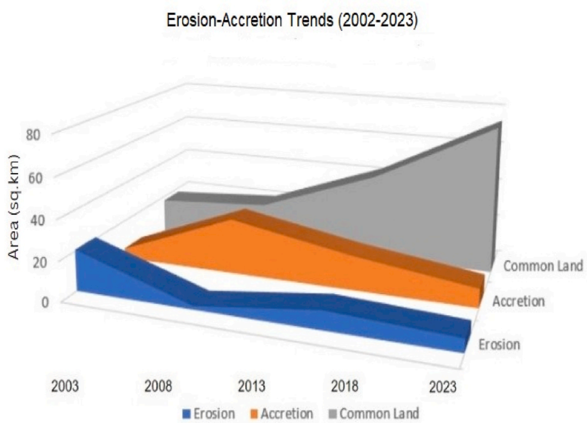

Fig. 5. Erosion-Accretion trend of Bhasan Char (2003–2023).

to water inundation. The slope, flow direction, and proximity to the shore are integrated to generate inland patches for different surge height scenarios, representing increasing flood severity. A weighted overlay analysis is performed by combining elevation, slope, distance from shore, and flow direction layers with calibrated weightings, resulting in a composite risk map that highlights areas of varying vulnerability [Fig. 4]. The final output is an inundation map showing inland regions categorized by their susceptibility to storm surge flooding, which provides valuable insights for coastal management and disaster risk mitigation. The methodology incorporates adjustments such as localized topographic variations and historical surge data to improve model accuracy and reflect specific regional vulnerabilities, making it an effective tool for predicting inundation risk.

Table 2
Erosion-Accretion summary of Bhasan Char Island (2003–2023).

Duration	Erosion (km^2)	Accretion (km^2)	Common Land (km^2)
2003–2008	20.82	5.13	17.72
2008–2013	1.75	28.15	21.75
2013–2018	9.27	17.52	43.57
2018–2023	6.49	9.43	74.34

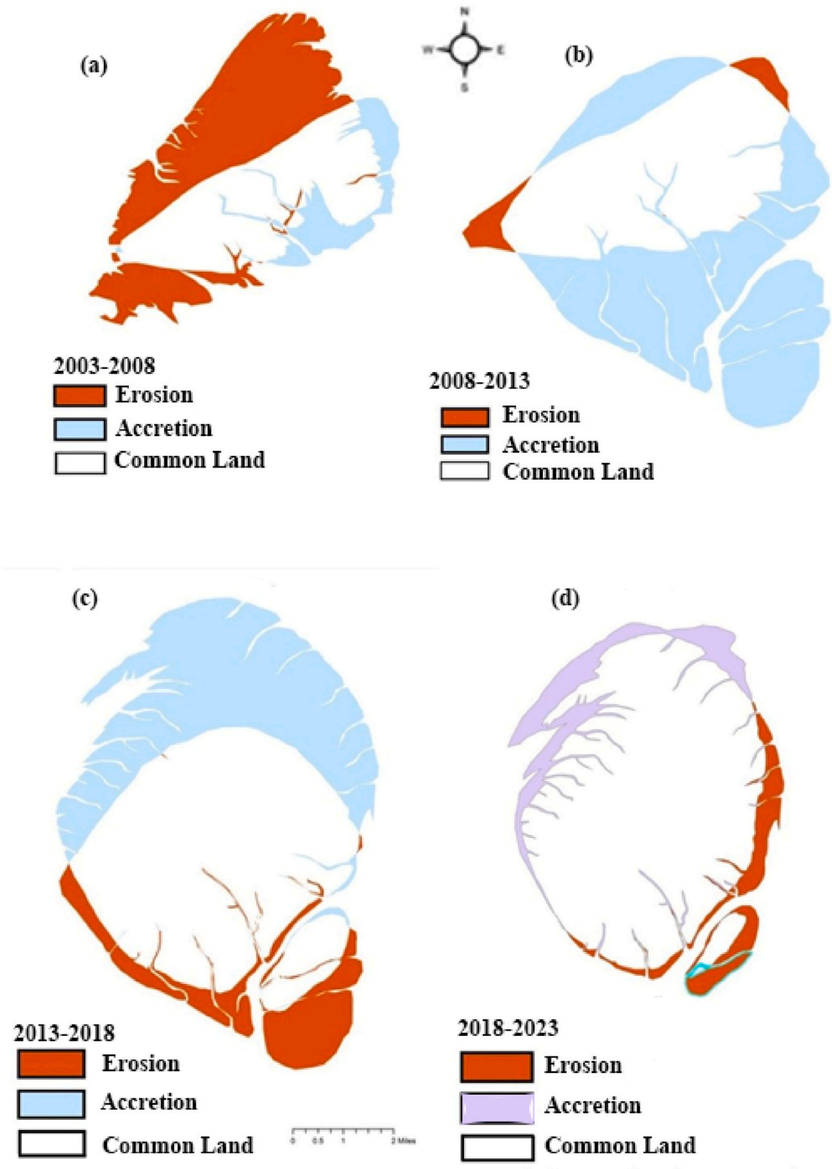

Fig. 6. Erosion-Accretion synopsis of Bhasan Char Island between the years of (a) 2003 and 2008, (b) 2008 and 2013, (c) 2013 and 2018, and (d) 2018 and 2023.

4. Results and discussion

4.1. Geomorphic dynamics analysis

The geomorphology of the Bhasan Char Island has observed a huge change over time for the past 20 years in this study. It includes

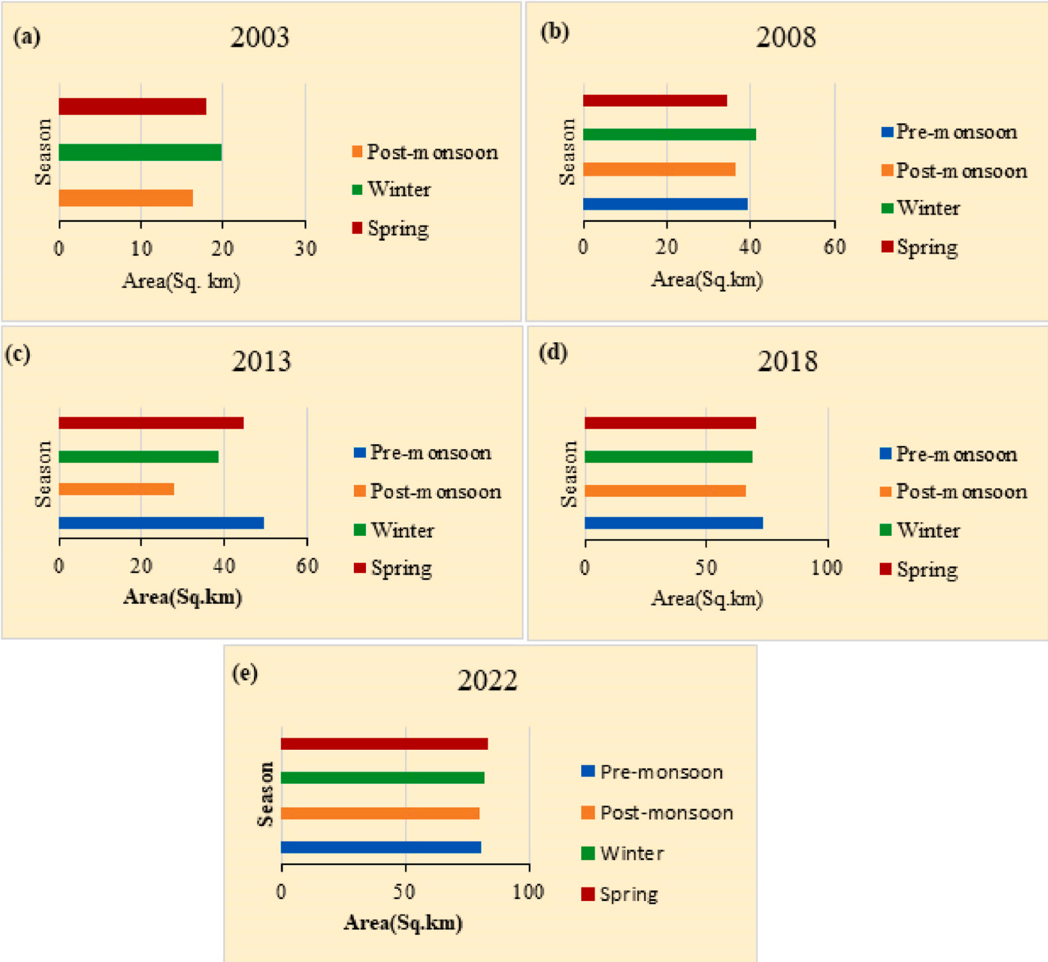

Fig. 7. Seasonal areal change of Bhasan Char Island; (a) highest in winter and lowest in post-monsoon at 2003, (b) highest in winter and lowest in pre-monsoon at 2008, (c) highest in spring and lowest in post-monsoon at 2013, (d) highest in spring and lowest in post-monsoon at 2018, (e) highest in pre-monsoon and lowest in post-monsoon at 2022.

dynamics of land erosion-accretion, area, shape of island and shoreline due to seasonal changes. There are approximately 70 islands close to and offshore from Bangladesh's coastal region. The island of Bhasan Char is located in the center of the coastal belt. The majority of the islands in the Meghna estuary were created by the silt that the GBM river system carried. The Meghna estuary is the most active location for the deposition and reworking of silt [33].

4.2. Erosion-accretion dynamics

The offshore islands of Bangladesh have continuously been modified by the erosion-accretion process [34]. Due to the prevalent erosion-accretion processes, the area is quite active. In Bangladesh's coastal region, tropical cyclones are a frequent cause of catastrophe. The center portion of the coastline area is a little bit safer than the eastern and western parts [35,36]. Generated from sediments driven by the GBM, the Bhasan Char Island is situated at the Meghna estuary of the GBM river system. Because of the location's rich sediment supply and the complex interactions between the material and the ocean, erosion, and accretion are frequently evolving phenomena. For more than 20 years, erosion and accretion have occurred simultaneously in certain areas of the island [Fig. 5]. Over the study period, we observed an increasing trend of stable land as common in the change detection analysis of two years (Table 2).

The temporal evaluation spans a five-year interval from 2003 to 2023, revealing dynamic changes in the island's landmass [Fig. 6]. Between 2003 and 2008, the island, with a common land area of 17.72 km^2, experienced substantial erosion of 20.82 km^2 and simultaneous accretion of 5.13 km^2, marking the highest erosion rate. Notably, the northern portion experienced substantial erosion due to the lack of barriers against the force of the Meghna River. From 2008 to 2013, the island grew significantly, developing a head-and-tail shape with little erosion. Over the next five years (2013–2018), erosion outpaced accretion, as the northern region experienced accretion and the southern region saw erosion. According to this study (2018–2023), the island degraded 6.49 km^2 and accreted 9.43 km^2, primarily in the northwestern and south-eastern sections. Despite variations, the common land area expanded to 74.34 km^2

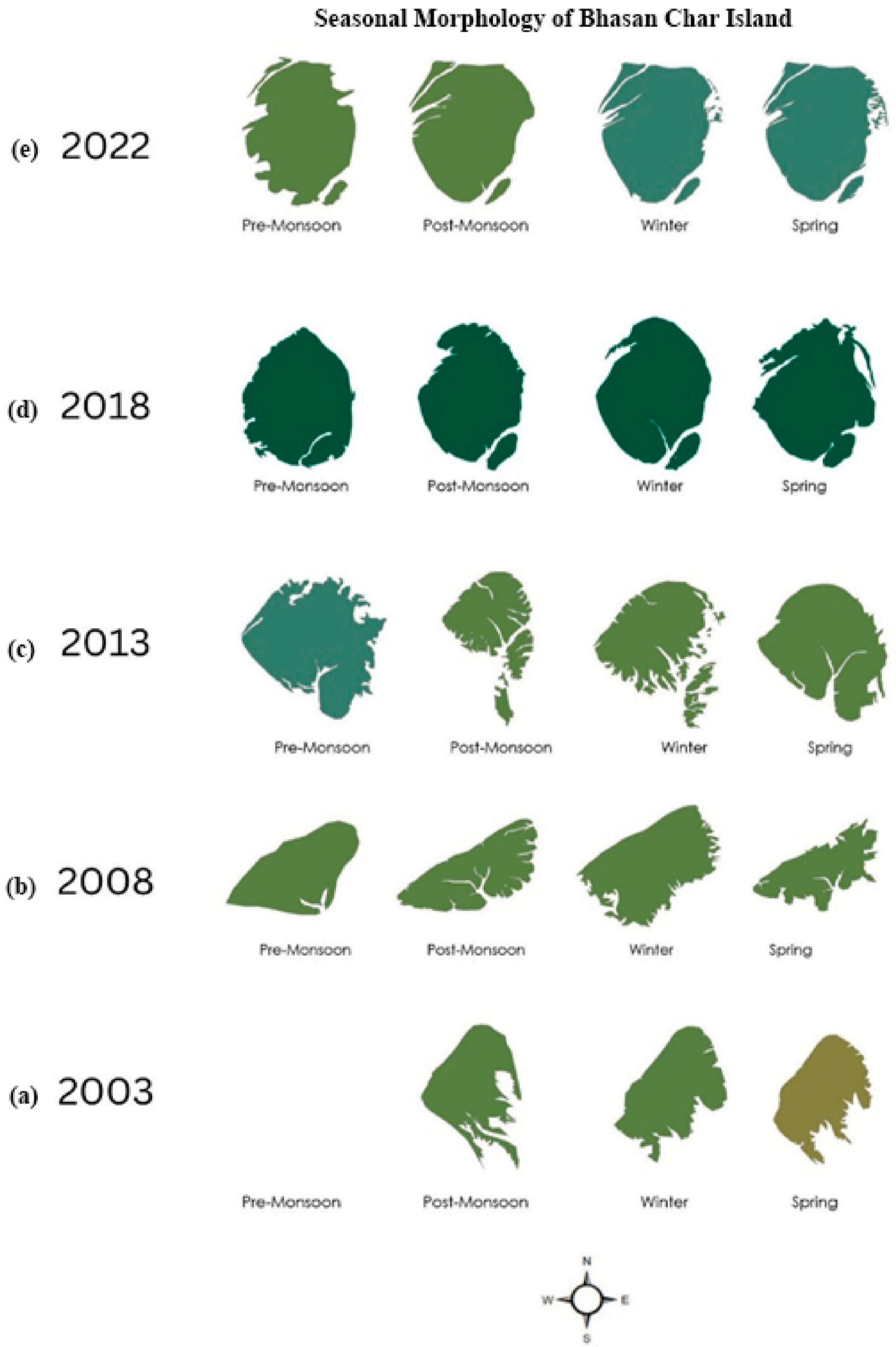

Fig. 8. Morphological seasonal variation of Bhasan Char Island for the five years' interval from 2003 to 2022 as shown in the panel (a) to (e) respectively.

over the recent decade, demonstrating increasing stability.

4.3. Variation of land area

Between 2003 and 2022, the evaluation of changes in land area due to seasonal variations was carried out [Figs. 7 and 8]. Pre-monsoon (late April–May), post-monsoon (September–October), winter (late December–January), and spring (March) were the four seasons of the year. Variations in wave and tide action, local sea level fluctuations, temperature changes causing morphological changes in the water bodies around the island, and other factors all impact the morphological changes on the island during each

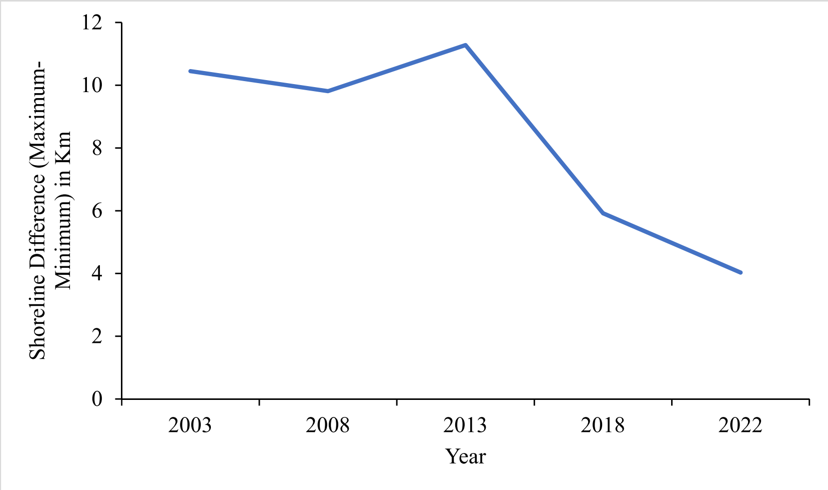

Fig. 9. Trend of shoreline change of Bhasan Char Island from 2003 to 2022.

season.

In 2003, the winter season had the most land area (19.79 km^2) while the post-monsoon season had the least (16.29 km^2). As a result, the areal extent peaked in the winter and decreased in the post-monsoon season. In 2008, the land area was greatest in the winter and least in the post-monsoon season. In 2013, the pre-monsoon season had the most land area, while the post-monsoon season had the least. This year saw the greatest shift in the land area because the tail of the island had almost submerged owing to seasonal variations. In 2018, the spring season had the most land area and the post-monsoon season had the least, as tidal canals took up more acreage. The highest land area recorded in 2022 was spring (83.32 km^2) and the least land area was recorded in post-monsoon (79.81 km^2).

4.4. Shoreline dynamics

Between 2003 and 2022, the shoreline length underwent significant changes, starting at 11.27 km in 2003 and gradually expanding to 83.27 km by 2022 [Figs. 9 and 10]. The longest shoreline recorded was 83.27 km in 2022. Throughout this period, a thorough assessment of coastline variations attributed to seasonal changes was conducted, with each year divided into four seasons: pre-monsoon (late April–May), post-monsoon (September–October), winter (late December–January), and spring (March). The fluctuations in shoreline morphology during each season are influenced by factors like wave and tide action, local sea level rise, temperature changes causing morphological shifts in water bodies around the island, and various other elements.

The longest shoreline occurred in winter (21.72 km) and the smallest in spring (11.27 km) in 2003, with prominent changes in the southeastern region from September to January. The shoreline had more than fivefold grown by 2008 due to significant accretion and low erosion. In 2008, the longest beachfront (44.45 km) was in the winter. During March–September 2013, modifications occurred in the south-eastern tail part, with the longest shoreline in pre-monsoon (47.53 km). By 2018, the island had changed shape to a sub-rounded shape, indicating greater stability. In 2022, coastline changes, particularly in the south-eastern region from March to September, resulted in the longest shoreline in spring (83.27 km) and the shortest in post-monsoon (79.24 km), resulting in a length difference of 4.03 km. By comparing the length difference between the shortest and longest shortest shoreline in each year, a decrease in the difference after 2013 is noticed. That indicates that the island is gradually becoming less affected by seasonal change and their factors (wave action, tidal action, local sea level change, the change in temperature resulting in the morphological change in the waterbodies in and around the island, etc.). The island also possesses the shortest shoreline in post-monsoon (2003 being an exception) which is indicative of the loss in landmass due to excessive rainfall, local sea level rise, and stronger tidal and wave action during that specific season.

The intensity of these alterations is decreasing even while the island continues to experience erosion-accretion, coastline change, and other geogenic modifications. The island's southwestern region appears to be the most stable and change-resistant, whereas the island's eastern region appears to be the most unstable. The spatiotemporal analysis indicates a change in the shape of the island. The island changed its elongated head-and-tail shape that had been observed in 2008 to a rounded to sub-rounded shape which has appeared in recent times. The island is now acquiring more territory than it did in earlier decades. Similar to its neighboring Hatiya and Sandwip Islands, the island will soon develop into a stable landmass. The geomorphic dynamics study (Shoreline change, areal extent change, and erosion-accretion) also indicates that the stability of the island has increased over time as it is less affected by seasonal variation than before.

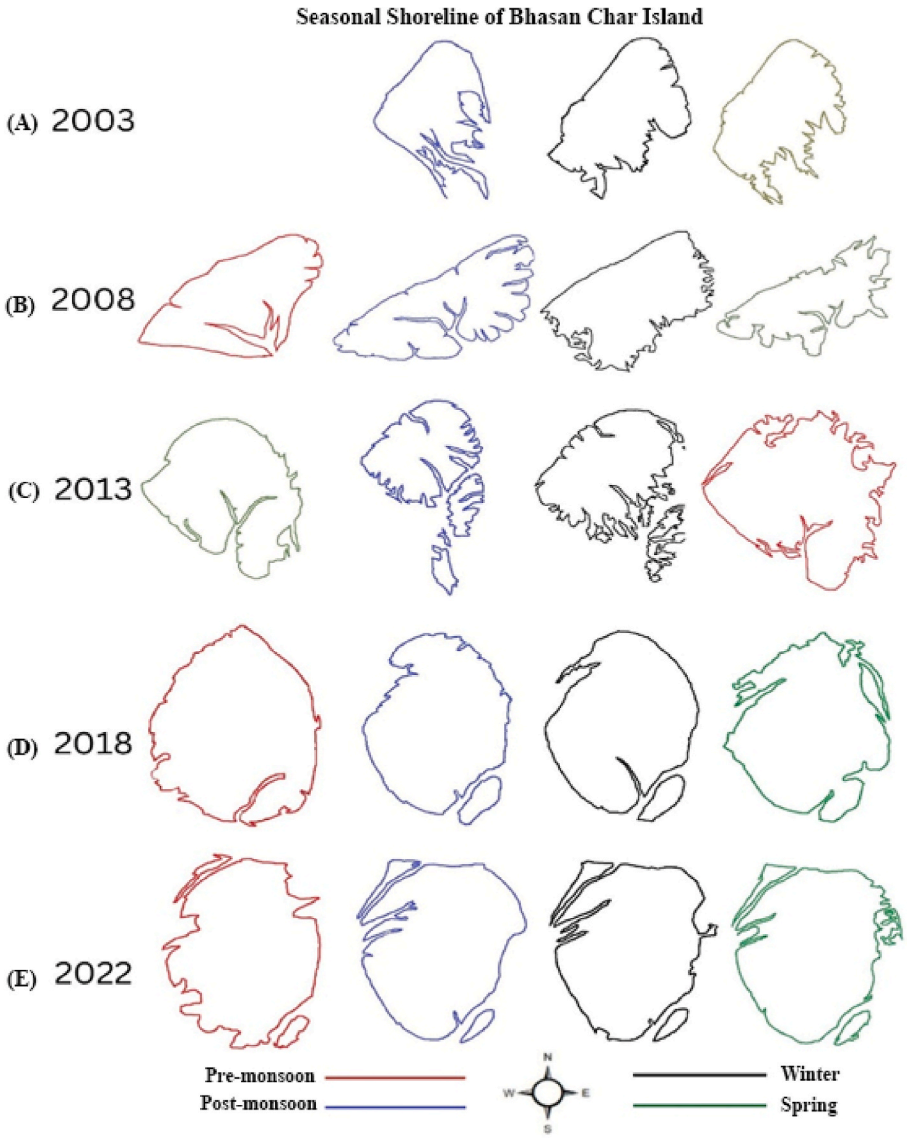

Fig. 10. Shoreline variation due to seasonal change of Bhasan Char Island for the five years' interval from 2003 to 2022 as shown in the panel (A) to (E) respectively.

4.5. Landuse-landcover dynamics

The landuse-landcover study of Bhasan Char island from 2003 to 2023 demonstrates a progressive shift [Fig. 11]. The spatio-temporal shift happened in two stages. The first phase, which lasted from 2003 to 2017, consisted of three components: a water body, vegetation, and grassland. The second phase began in 2017 with the construction of a helipad on March 14, 2017, followed by the establishment of shelters, mosques, factories, and purification plants. In this phase, more land clearance for agricultural reasons, such as fish farming, poultry, and vegetable production, extended the land use-landcover components, introducing settlement and agriculture to the island's landscape. Bhasan Char had a total land area of 19.79 km^2 in 2003, with vegetation covering 15.83 km^2, grassland covering 2.37 km^2, and an inland waterbody of 1.59 km^2. As a result, the areal covering was dominated by vegetation (91 %), with modest inland waterbodies (9 %) consisting of tidal channels and canals. vegetation (91 %) and minor inland waterbodies (9 %) which were tidal channels and canals.

The broad grasslands were the island's primary geographical feature between 2008 and 2018. In 2008, the total land area was 41.12 km^2, with vegetation accounting for 8.22 km^2, grassland contributing to 28.38 km^2, and inland waterbodies accounting for 4.52 km^2 [Fig. 12]. The vegetation dominated the environment, accounting for 89 % of the land covering, with inland waterbodies expanding inland due to tidal channels accounting for the remaining 11 %. In 2013, the total land area of the island was 49.53 km^2 of which vegetation covered 14.36 km^2, grassland covered 29.23 km^2, and inland waterbody covered 5.84 km^2. The island was still

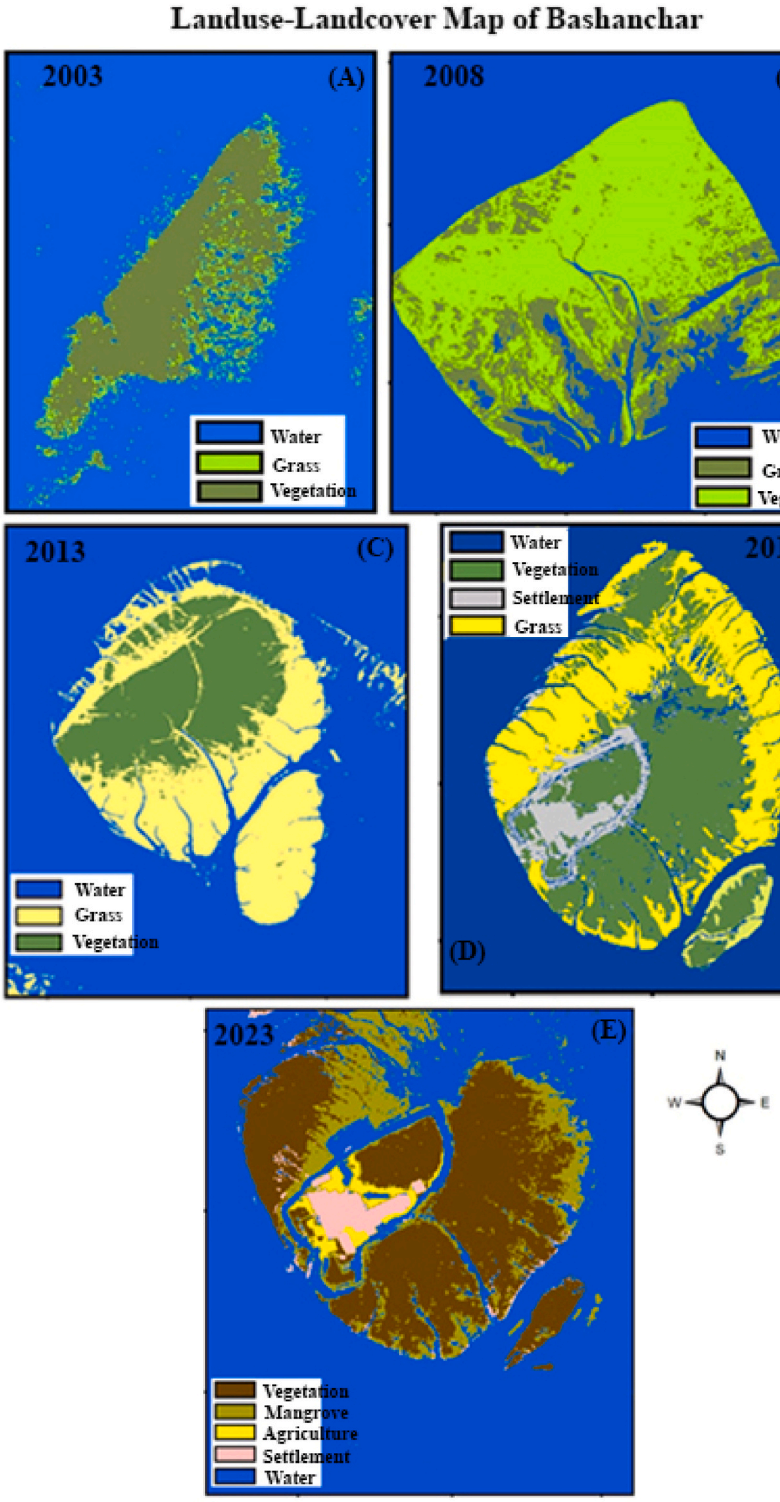

Fig. 11. Spatiotemporal changes of LULC of Bhasan Char for the five years' interval from 2003 to 2023 as shown in the panel (A) to (E) respectively.

majorly occupied by vegetation (88 %) with inland waterbodies (12 %). The Island's total land area increased to 68.95 km^2 in 2018, with diverse land-use components. Vegetation covered 23.44 km^2, grassland 35.16 km^2, inland water bodies 4.23 km^2, and settlement was discovered for the first time, encompassing 5.52 km^2. The addition of settlement to the land-use map began in 2018, coinciding

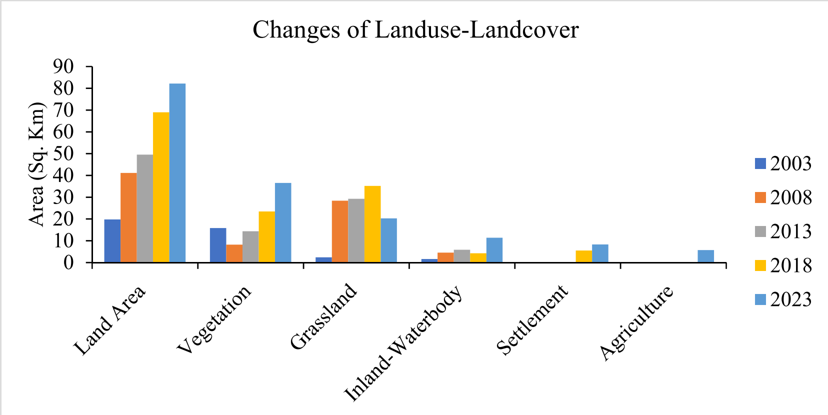

Fig. 12. Temporal changes of LULC from 2003 to 2023 in Bhasan Char island.

Fig. 13. Ground data collection point for accuracy assessment of the prepared LULC components of Bhasan Char; (a) is a pond inside the island representing waterbody class, (b) includes urban structure and grassland class, (c) shows the dense vegetation class along with presence of large water body, (d) is a residential area representing dense settlement, (e) shows the presence of current embankments within the island.

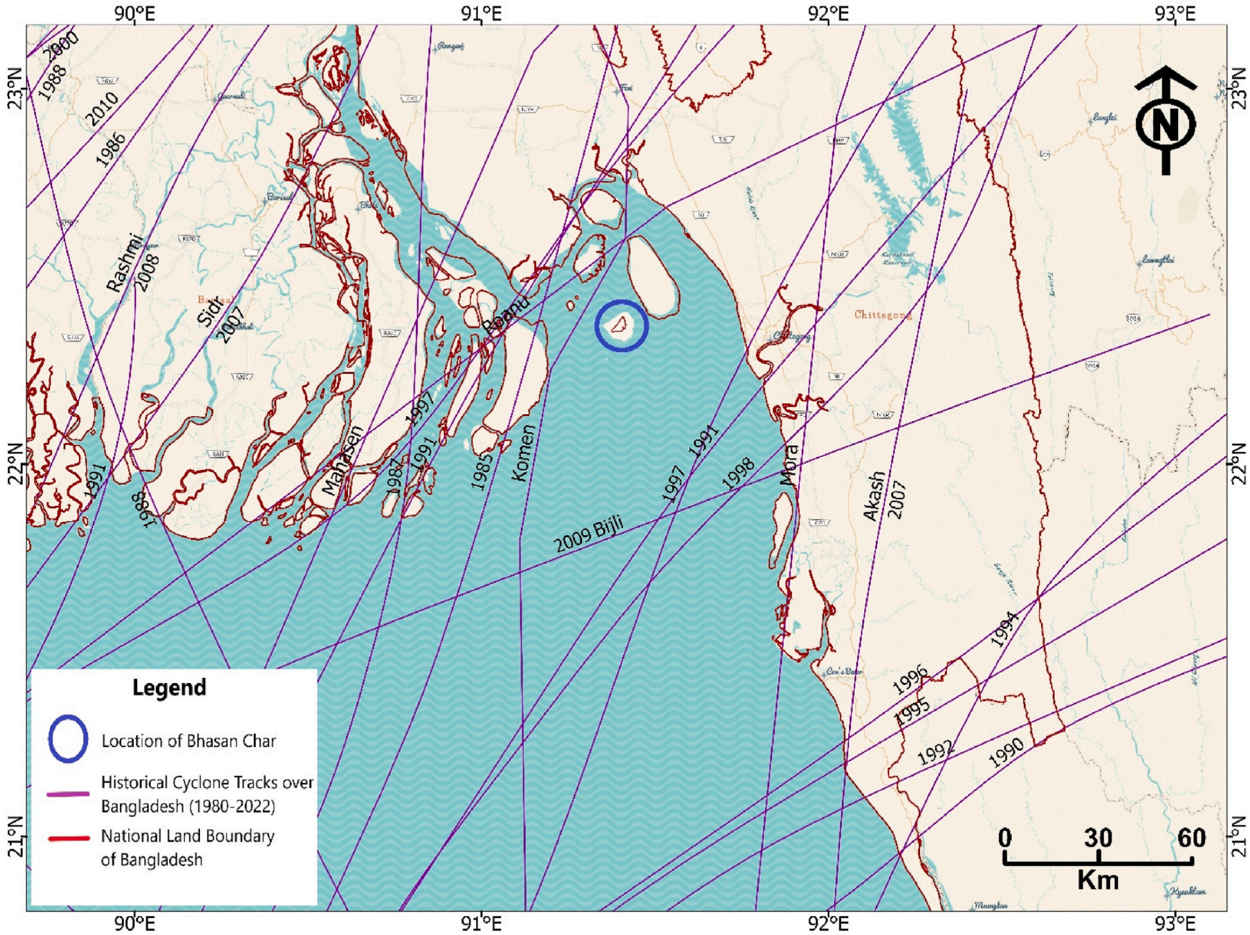

Fig. 14. Historical cyclone tracks (1980–2022) where the blue circle outlines the region of interest (Modified after [15]).

with the start of infrastructural work in 2017. This shift in land use and the cover was led by collaborative efforts by the government, non-governmental organizations, and corporate entities in Bangladesh and around the world, with a special emphasis on the island's rehabilitation program for FDMN (Forcibly Displaced Myanmar Nationals). Despite these changes, the island was still mostly populated by vegetation (84 %), inland water bodies (6 %), and settlements (10 %). In 2023, the island's total land area is 82.15 km^2, with vegetation covering 36.51 km^2, grassland covering 20.28 km^2, inland-waterbody, mostly ponds [Fig. 13 (a)] and narrow khal [Fig. 13 (c)] covering 11.36 km^2, settlement covering 8.28 km^2, and agricultural covering 5.72 km^2. In 2023, vegetation dominated the land area, and agriculture was introduced as a new component to the landuse-landcover map. The 'Ashrayan-3′ project, which aimed to relocate 100,000 FDMN to the island, resulted in substantial urbanization on the island. Vegetation covered 69 % of the island, with inland waterbodies accounting for the remaining 13 %. In the last five years, the tidal channels have sliced further into the island. The settlement took up 10 % of the region. Agriculture was first identified in the 2023 landuse assessment, where it occupied 7 % of the island. The settlement includes homes, cyclone shelters, mosques, schools, a graveyard, hospitals, a buffalo farm, a stadium, garments, treatment plants, stove repairing centers, a lighthouse, a VIP guest house [Fig. 13 (b)], hotels [Fig. 13 (d)], sluice gates [Fig. 13 (e)], bazaars, departmental stores, playing fields and an embankment of 5.8m height surrounding all the settlements. The agricultural land includes agricultural ponds for fish cultivation by BRAC and Caritas, a lake farm project by MSI, ACLAB agro-village, etc.

4.6. Surge inundation risk of Bhasan Char

The majority of past tropical cyclones struck Bangladesh from the southwest toward the northeast; the south-central communities are the most vulnerable [Fig. 14]. Cyclone surges inundate low places along the coast; as the distance from the shore rises, the islands are pretty impacted. Along with the research, the findings highlight the likely susceptible conditions of the Bhasan Char, which is very sensitive to storm surges during high-amplitude cyclones. On the Bhasan Char Island, the effects of cyclones, sea level rise, and climate change are not as severe as they are on the adjacent islands.

The possible impact of storm surges on the island varies depending on the height of the surge. The impacts of surges ranging from 1 to 3 m are comparable, with inundation of low-elevation barren regions along the southern margins, affecting roughly 37 % of such

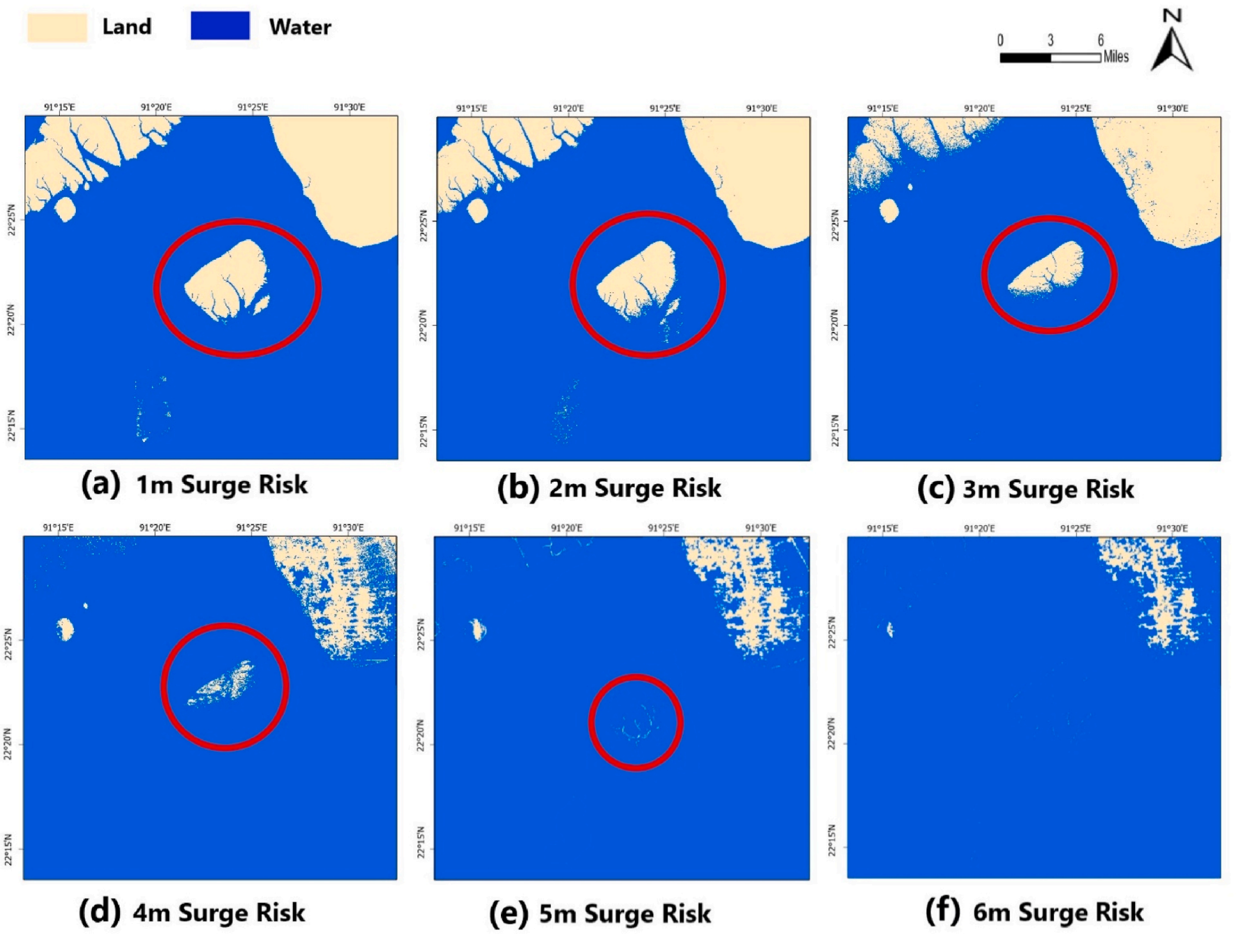

Fig. 15. Storm Surge Inundation Risk Map of Bhasan Char for storm surges ranging from 1m to 6m as shown in panel (a) to (f) respectively.

places [Fig. 15(a–c)]. Even though the island's average elevation is 2.84 m above mean sea level, a surge height of 3–4 m offers a severe flooding risk, burying significant portions of the island [Fig. 15(d and e)]. Surges of more than 3 m, especially above 4 m, might inundate more than 67 % of the southern lands. Settlement communities are extremely vulnerable, especially if surge heights exceed 5 m, which might affect the population living within a 4.8-m embankment built as part of the 'Ashrayan-3′ project. This embankment, which has a steady slope angle and sluice gates, was built to safeguard towns and agricultural regions, however, heights above 5 m pose a direct threat to the settlement within the embankment [Fig. 15 (f)].

According to the storm surge inundation assessment, a 3m sea level rise would have little effect on Bhasan Char Island (Fig. 15). A 3–5m storm surge, on the other hand, might impact the outer embankment, creating environmental and human dangers. If the surge exceeds 5m, the island might face disastrous repercussions. With a significant freshwater supply from deep subsurface aquifers, the island employs defensive measures such as embankments, sluice gates, and wavebreakers. The government is preparing for the effects of climate change, governed by international treaties. Concerns over the migration of FDMN refugees to Bhasan Char remain, emphasizing the importance of sustainability and safety during natural disasters.

However, the study has limitations. The studied satellite images, Landsat TM, and OLI sensor images with a resolution of 30m were constrained by seasonal ranges and required low cloud coverage. During certain months, superior 10m resolution Sentinel photos were unavailable, affecting study accuracy. The provided Digital Elevation Model (DEM) was created using pre-4.8m embankment construction data surrounding the hamlet. Recent data collection may result in changes to the storm surge danger map. Having access to high resolution Sentinel satellite images may have improved study precision. Despite these limitations, the study gives useful insights into the dynamics of the island, emphasizing the importance of extensive data and technological considerations in future studies.

5. Conclusion

The focus of the research is on assessing Bhasan Char Island in light of morphological changes, changes in landuse-landcover, and risk evaluation of storm surge inundation. Sustainable rehabilitation is not possible without guaranteeing environmental safety about the geological stability and environmental stability. Bhasan Char Island has grown seven times in the last two decades, adding 66 km^2

since 2003. Recent accretion rates throughout the shoreline, particularly in the east, have exceeded erosion rates, indicating greater stability. Notably, the island has changed shape from elongated to sub-rounded and is now rounded (9 km × 8 km). Since 2017, the FDMN rehabilitation project has resulted in a decrease in vegetation and an increase in settlement and agricultural land. The current embankment height of 4.8 m is judged adequate to protect against heavy storm surges. Overall, the island has grown structurally, morphologically, and in size, demonstrating enhanced stability in the face of coastal modification and cyclone dangers. These changes are critical for the FDMN population's future environmental safety. The island is gradually expanding, becoming more stable, safer, and sustainable for the FDMN population's interim rehabilitation. This work is an important global case study, advising academics and policymakers to do extensive geo-environmental assessments before embarking on island restoration efforts. While the current stability forecast is based on a short timescale, validation needs to take other geological and environmental aspects into account. The installation of groins across the island can help to accelerate the natural accretion process. Ensuring that the island's restored population is compatible with its natural environment, is a vital priority in light of increased settlement.

CRediT authorship contribution statement

Mubtasim Ishraq Antoo: Writing – original draft, Visualization, Validation, Methodology, Investigation, Formal analysis. **Md. Bodruddoza Mia:** Writing – review & editing, Supervision, Project administration, Methodology, Conceptualization. **Md. Asif Hasan:** Writing – review & editing, Validation, Software, Methodology, Formal analysis. **Mahfuzur Rahman Khan:** Visualization, Validation, Resources, Funding acquisition, Conceptualization. **Pavel Khan:** Writing – review & editing, Resources, Project administration, Investigation, Data curation. **Tareq Chowdury:** Writing – review & editing, Validation, Supervision, Resources, Project administration. **Anupom Hasib Rose:** Writing – original draft, Visualization, Resources, Formal analysis. **Kazi Matin Uddin Ahmed:** Writing – review & editing, Supervision, Funding acquisition, Conceptualization.

Data availability statement

Data will be made available on request.

Declaration of competing interest

The authors declare the following financial interests/personal relationships which may be considered as potential competing interests: Md. Bodruddoza Mia reports financial support was provided by United Nations Children's Fund Bangladesh. If there are other authors, they declare that they have no known competing financial interests or personal relationships that could have appeared to influence the work reported in this paper.

Acknowledgement

This work is an outcome of a MS research. The research was supported by the funding of Dhaka University-UNICEF research grant.

References

[1] UNHCR, Press statement: united nations statement on the relocation of Rohingya refugees to bhasan char. https://reliefweb.int/report/bangladesh/press-statement-united-nations-statement-relocation-rohingya-refugees-bhasan-char, 2020. (Accessed 10 February 2021).
[2] ICJ, Application of the Convention on the Prevention and Punishment of the Crime of Genocide (The Gambia V. Myanmar), 2020.
[3] S. Zaman, P. Sammonds, B. Ahmed, T. Rahman, Disaster risk reduction in conflict contexts: lessons learned from the lived experiences of Rohingya refugees in Cox's Bazar, Bangladesh, Int. J. Disaster Risk Reduc. 50 (2020) 101694.
[4] G. Donchyts, F. Baart, H. Winsemius, N. Gorelick, J. Kwadijk, N. Van De Giesen, Earth's surface water change over the past 30 years, Nat. Clim. Change 6 (9) (2016) 810–813.
[5] P.S. Kench, R.W. Brander, K.E. Parnell, R.F. McLean, Wave energy gradients across a Maldivian atoll: implications for island geomorphology, Geomorphology 81 (2006) 1–17.
[6] J.H. Nienhuis, A.D. Ashton, D.A. Edmonds, A.J.F. Hoitink, A.J. Kettner, J.C. Rowland, T.E. Törnqvist, Global-scale human impact on delta morphology has led to net land area gain, Nature 2020 577 (7791 577) (2020) 514–518, https://doi.org/10.1038/s41586-019-1905-9.
[7] H. Brammer, Bangladesh's dynamic coastal regions and sea-level rise, Climate risk management 1 (2014) 51–62.
[8] M.S. Hossain, J.A. Dearing, M.M. Rahman, M. Salehin, Recent changes in ecosystem services and human well-being in the Bangladesh coastal zone, Reg. Environ. Change 16 (2016) 429–443.
[9] M.G.M. Sarwar, C.D. Woodroffe, Rates of shoreline change along the coast of Bangladesh, J. Coast Conserv. 17 (2013) 515–526.
[10] A.H. Dolan, I.J. Walker, Understanding vulnerability of coastal communities to climate change related risks, Journal of Coastal research (2006) 1316–1323.
[11] R.E. Al-Haddad, K.L. Duran, S. Ahmed, A lost generation: perpetual education insecurity among the Rohingya, Race Ethn. Educ. 25 (6) (2022) 874–900.
[12] M.Y. Gazi, A.S.M. Kamal, M.N. Uddin, M.A.H. Bhuiyan, M.Z. Rahman, The stability and suitability of the Bhasan Char Island as an accommodation for the forcibly displaced Myanmar nationals (FDMN), Sustainability 14 (2) (2022) 747.
[13] P. Chakma, A. Akter, Flood mapping in the coastal region of Bangladesh using sentinel-1 SAR images: a case study of super cyclone amphan, J. Civil Eng. Forum 7 (3) (2021) 267, https://doi.org/10.22146/jcef.64497.
[14] N.M. Ha-Mim, A. Rahman, Z. Hossain, J.N. Fariha, K.R. Rahaman, Employing multi-criteria decision analysis and geospatial techniques to assess flood risks: a study of Barguna district in Bangladesh, Int. J. Disaster Risk Reduc. 77 (2022) 103081, https://doi.org/10.1016/j.ijdrr.2022.103081.
[15] M.A. Hasan, A.N. Mayeesha, M.Z.A. Razzak, Evaluating geomorphological changes and coastal flood vulnerability of the Nijhum Dwip Island using remote sensing techniques, Remote Sensing Applications Society and Environment 32 (2023) 101028, https://doi.org/10.1016/j.rsase.2023.101028.
[16] A. Islam, S. Hossain, S. Murshed, Assessment of coastal vulnerability due to sea level change at Bhola island, Bangladesh: using geospatial techniques, J. Indian Soc. Remote Sens. 43 (3) (2015) 625–637, https://doi.org/10.1007/s12524-014-0426-0.

[17] M.R.A. Mullick, A.H. Tanim, S.M.S. Islam, Coastal vulnerability analysis of Bangladesh coast using fuzzy logic based geospatial techniques, Ocean Coast Manag. 17M.A. Hasan et al. Remote Sensing Applications: Society and Environment 32 (101028 174) (2019) 154–169, https://doi.org/10.1016/j.ocecoaman.2019.03.010, 2023.

[18] N. Bushra, R.B. Mostafiz, R.V. Rohli, C.J. Friedland, M.A. Rahim, Technical and social approaches to study shoreline change of kuakata, Bangladesh, Front. Mar. Sci. 8 (2021) 730984, https://doi.org/10.3389/fmars.2021.730984.

[19] S. Roy, R. Mahmood, Monitoring shoreline dynamics using Landsat and hydrological data: a case study of Sandwip island of Bangladesh, Penn. Geogr. 54 (2) (2016) 20–41.

[20] J. Helgeson, C. O'Fallon, Resilience dividends and resilience windfalls: Narratives that tie disaster resilience co-benefits to long-term sustainability, Sustainability 13 (8) (2021) 4554.

[21] S. Bagli, P. Soille, Morphological automatic extraction of pan-European coastline from Landsat ETM + image, Proceeding ofThe 5th International Symposium on GIS and Computer Cartography for Coastal Management, Genova, 26 September 2003 (2003) 58–69.

[22] A.S. Genz, C.H. Fletcher, R.A. Dunn, L.N. Frazer, J.J. Rooney, The predictive accuracy of shoreline change rate methods and alongshore beach variation on Maui, Hawaii, J. Coastal Res. 231 (2007) 87–105.

[23] M. Bouchahma, W. Yan, Automatic measurement of shoreline change on Djerba Island of Tunisia, Comput. Inf. Sci. 5 (5) (2012) 17.

[24] L. Bremner, Sedimentary logics and the Rohingya refugee camps in Bangladesh, Polit. Geogr. 77 (2020) 102109.

[25] Y. Cowper-Smith, The bhasan char relocation project–implications for Rohingya refugees in Bangladesh, Relief Web (2020).

[26] N. Menon, Urban sprawl—a developing country approach. WSCSD, Yale University, 2004.

[27] M.S. Islam, Assessing the dynamics of land cover and shoreline changes of Nijhum Dwip (Island) of Bangladesh using remote sensing and GIS techniques, Regional Studies in Marine Science 41 (2021) 101578.

[28] S.K. McFeeters, The use of the Normalized Difference Water Index (NDWI) in the delineation of open water features, Int JRemote Sens 17 (7) (1996) 1425–1432, https://doi.org/10.1080/01431169608948714.

[29] H. Xu, Modification of normalised difference water index (NDWI) to enhance open water features in remotely sensed imagery, Int. J. Rem. Sens. 27 (14) (2006) 3025–3033.

[30] A. Emran, M.A. Rob, M.H. Kabir, et al., Modeling spatio-temporal shoreline and areal dynamics of coastal island using geospatial technique, Model. Earth Syst. Environ. 2 (2016) 4, https://doi.org/10.1007/s40808-015-0060-z.

[31] M.A. Islam, D. Mitra, A. Dewan, S.H. Akhter, Coastal multi-hazard vulnerability assessment along the Ganges deltaic coast of Bangladesh–A geospatial approach, Ocean Coast Manag. 127 (2016) 1–15.

[32] Md Asif Hasan, Md Nazim Uddin, Yousuf Gazi, Surge modelling and inundation mapping of the cyclone-prone island districts of Bangladesh using geospatial and remote sensing techniques, International Conference on Earth & Environmental Sciences and Technology, Dhaka. Conference Proceedings 1 (2020) 544–545, https://doi.org/10.13140/RG.2.2.23175.27045.

[33] M.S. Iftekhar, Conservation and management of the Bangladesh coastal ecosystem: overview of an integrated approach, InNatural Resources Forum; Blackwell Publishing Ltd: Oxford, UK 30 (2006) 230–237.

[34] M.S. Alam, K. Uddin, A study of morphological changes in the coastal areas and offshore islands of Bangladesh using remote sensing, Am. J. Geogr. Inf. Syst. 2 (1) (2013) 15–18.

[35] M.F. Karim, N. Mimura, Impacts of climate change and sea-level rise on cyclonic storm surge floods in Bangladesh, Glob. Environ. Change 18 (2008) 490–500.

[36] U. Haque, M. Hashizume, K.N. Kolivras, H.J. Overgaard, B. Das, T. Yamamoto, Reduced death rates from cyclones inBangladesh: what more needs to be done? Bull. World Health Organ. 90 (2012) 150–156.